Theor Chem Acc (2000) 105:39–45
DOI 10.1007/s002140000177

Theoretical
Chemistry Accounts

Regular article

A density functional theory study of the conformational properties of 1,2-ethanediamine: protonation and solvent effects

David De Corte, Carl-Wilhelm Schläpfer, Claude Daul

Institute of Inorganic and Analytic Chemistry, University of Fribourg, 1700 Fribourg, Switzerland

Received: 28 September 1999 / Accepted: 2 May 2000 / Published online: 27 September 2000

Abstract. The structures and the conformational energies of nonprotonated, monoprotonated and diprotonated 1,2-ethanediamine have been investigated through density functional theory. The relative performance of local and gradient-corrected functionals is discussed. The existence of hydrogen-bond formation has been determined with electron localisation function calculations. Proton affinities for nonprotonated and monoprotonated 1,2-ethanediamine have been calculated and are in agreement with experimental data. The influence of solvation has been accounted for through the self-consistent isodensity polarisable continuum model. The results for the nonprotonated conformers show that solvation stabilises those conformers which have the lone pair in an antiperiplanar conformation. Solvation of the monoprotonated conformer stabilises significantly the ''anti'' conformation, which is unstable in the gas phase. For the di-protonated species, solvation stabilises slightly the gauche conformer, which is unstable in the gas phase.

Key words: Density functional theory – Solvation – Protonation – Electron localisation function

1 Introduction

A lot of work on the stability of metal complexes with mono- and polydentate ligands has been carried out in the last 50 years. In the complex formation, not only the geometries of the complexes formed are important, but also the conformational properties of the free ligands, i.e. we have to know if the polymer backbone is able to adapt to the structural requirements of the metal ion without strain. In this study we discuss the influence of protonation and solvation on the conformational properties of the ligand 1,2-ethanediamine (EDA), which is a building block of polyethylenimine [1].

Electron diffraction experiments [2] in the gas phase have shown that nonprotonated EDA is predominantly (95%) in a gauche conformation with a dihedral angle φ_{NCCN} of 64(5)° and r_{CC} and r_{NC} bond lengths of 1.545(8) and 1.469(4) Å, respectively. Moreover, microwave spectroscopy [3] showed that in the dominant gauche form, one of the NH_2 groups may assume either of two positions, depending on the hydrogen atom involved in the hydrogen bonding. It is found that φ_{NCCN}, r_{CC} and r_{NC} are 63(2)°, 1.546 and 1.469 Å, respectively. No structural data are available for the monoprotonated EDA (EDA1) and diprotonated EDA (EDA2) species, either in the gas phase or in aqueous solution.

A lot of theoretical work has also been performed in order to investigate the conformational properties of nonprotonated EDA in the gas phase. These studies include empirical [5], semiempirical [1, 6–7] and non-empirical [8–12] calculations, which give not only detailed information about the most stable structural conformers, but also their relative energies and their electronic properties. The factors stabilising the gauche conformers are assumed to be both what is called the ''gauche effect'' and intramolecular hydrogen bonding between the two amine groups. Kazerouni and Hedberg [9] estimated a 0.84 kJ mol^{-1} stabilisation through the gauche effect. Sang and Mhin [10] proposed a 4.6 kJ mol^{-1} stabilisation through the hydrogen bond and a 10.0 kJ mol^{-1} destabilisation for the lone-pair repulsion.

Boudon and Wipff [13] studied EDA2 and also considered the effect of solvation on the conformational properties of EDA2, by including explicit water molecules in a molecular dynamics study.

None of these studies were done at the density functional level. Hence, the present density functional theory calculations are compared to both experimental and theoretical data, in the case of nonprotonated EDA. We predict the rotational energy surfaces and structural parameters of the EDA1 and EDA2 molecules, both in the gas phase and in aqueous solution. The proton

Correspondence to: C. Daul
e-mail: claude.daul@unifr.ch

affinities (PAs) of the nonprotonated EDA and the EDA1 conformers have also been calculated. The formation of hydrogen bonds is illustrated through electron localisation function (ELF) calculations [14, 15].

2 Computational methods

2.1 Density functional calculations

Density functional calculations were carried out using the Gaussian94 [16] and ADF23 [17] program packages. For the Gaussian94 calculations 4-31G* and 6-31G** basis sets were used. Both the local density approximation (LDA) [18] and the generalised-gradient approximation (GGA) functionals Perdew's 1986 gradient-corrected correlation functional with Becke's exchange functional (BP86) [19] and Becke's three parameter hybrid method with the Lee, Yang and Parr correlation functional (B3LYP) [20] were utilised. An aqueous solvent was included through the self-consistent reaction field (SCRF) model, such as the Onsager dipole model [21] and the self-consistent isodensity polarisable continuum model (SCIPCM) [22] available in Gaussian94. For the dipole model, a spherical cavity with a hydrophobic radius of 6.04 Å, obtained through a volume calculation of the molecule, and a dielectric constant of 80.0 for the solvent were used. Using the SCIPCM we considered the isodensity surface with a value of $\rho_{\text{lim.}} = 0.001$.

All ADF23 calculations were carried out using a triple-zeta Slater-type orbital basis set with one polarisation function and the core electrons of C(1*s*) and N(1*s*) were kept frozen. All ADF23 calculations were done at the nonlocal BP86 level. ELF calculations based on densities obtained from ADF23 calculations were used to show the presence of hydrogen bonds.

2.2 ELF as a tool to study bonding

The introduction of the ELF by Becke and Edgecombe in 1990 [14] has led to a quantitative tool to describe chemically intuitive concepts such as the chemical bond and electron pair. This function allows one to describe in a topological way a quantity related to the Pauli exclusion principle. The local maxima of this function define "localisation attractors", of which there are only three basic types: bonding, nonbonding and core. The spatial organisation of localisation attractors provides a basis for a well-defined classification of bonds. An obvious advantage of this function is that it can be derived from theory and experiment. Since this tool of bond analysis is not popular yet, we will give some computational details and guidelines.

2.2.1 The ELF implementation

The ELF was originally derived from the conditional probability of finding an electron of spin σ at $\mathbf{r}'$ when an electron with the same spin is at $\mathbf{r}$. As proposed by Becke and Edgecombe, ELF is a simple function taking values between 0 and 1 and measuring the excess local kinetic energy due to the Pauli repulsion.

For a single determinantal wavefunction built from Hartree–Fock or Kohn–Sham orbitals, φ_i, and an electron density, ρ^σ, the value $\text{ELF} = 1/1 + \left(\text{D}_\sigma/\text{D}_\sigma^0\right)^2$, where $\text{D}_\sigma = \frac{1}{2}\sum_{i=1}^{N} |\nabla\varphi_i|^2 - \frac{1}{8}|\nabla\rho^\sigma|^2/\rho^\sigma$ and $\text{D}_\sigma^0 = \frac{3}{10}(3\pi^2)^{2/3}\rho_\sigma^{5/3}$, is calculated on a grid in the three-dimensional space.

Usually the quantum chemical calculations give results that are nonlocal, quantitative, predictive and approximation-dependent. In the discussion of chemical bonds, chemists use arguments that are local, qualitative, explicative and approximation-independent. The ELF fills the gap by providing a mathematical definition of the bond as a local property of the matter. Furthermore, quantum mechanics is still valid in the definition, the property is available from theory and experiment and is close to the Lewis nomenclature. One main advantage is the independence of the ELF from the level of approximate theory used.

2.2.2 Properties of the ELF

The ELF can take values between 0 and 1. For regions where there is no localisation of electron pairs or for regions where electrons of the same spin are predominant, the ELF has a value close to 0. For regions where there is a high pair localisation and also in regions dominated by a single, localised electron, the ELF is close to 1. For a value of ELF = 0.5, the region is exactly of the electron-gas type. Isosurfaces of the ELF divide space into localisation domains. With topological arguments, Savin et al. [15] have classified the different types of regions of high values of the ELF or "attractors" as core, valence bonding, valence non-bonding, valence protonated and valence nonprotonated.

The ELF allows a more rigorous definition of the concept of a delocalised bond and nonbonding electron pairs: in both cases, one expects that the function reaches a higher value in a region where the Lewis structure predicts the presence of an electron pair (bonding or not).

3 Results and discussion

3.1 Nonprotonated EDA

In order to specify the different conformations of nonprotonated EDA, we use the following notations, as shown in Fig. 1: the symbols A(anti) and G(gauche) correspond to the arrangement of the amine groups about the C—C axis. Primes are used for angles greater than 180°. The symbols a, g and g′ refer to the orientations of L, the lone pair of the N atom, for which the dihedral angles are 180°, 60° and 300°, respectively.

As described by Sang and Mhin [10], we can then group all the conformers arising from different orientations of their lone pairs into four categories: aa; ag, ga, ag′, g′a; gg′, g′g; gg, g′g′. Thus, in order to analyse the complete rotational potential-energy surface, we only considered four conformers, i.e. the aa, ag′, gg′ and gg conformers of EDA.

The rotational energy profiles of these conformers shown in Fig. 2 are calculated with a 4-31G* basis set and BP86. Linear transit calculations were done through a continuous scan of φ_{NCCN} in steps of 10° and thereafter optimising the geometry with a frozen φ_{NCCN}

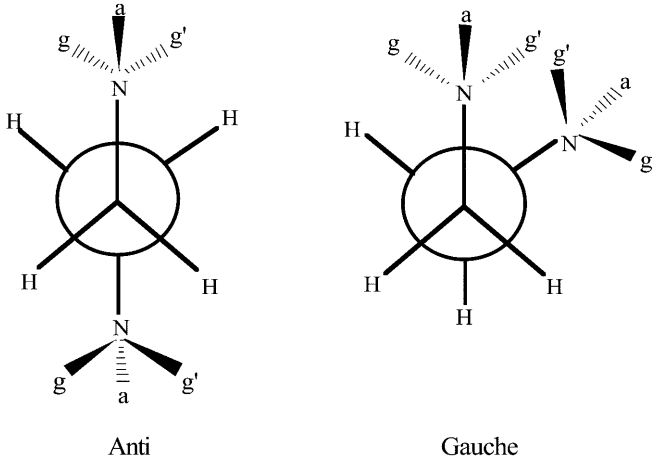

Fig. 1. Notation for the specification of the different conformations of 1,2-ethanediamine (*EDA*). The N lone pair electron orbital position is represented in three different conformations: *a*, *g* and *g*′

angle. For all four types of N lone pair orientations, we find structures with local energy minima corresponding to dihedral angles of 60°, 180° and 300°. We find energy maxima (transition states) at 0°, 120° and 240°. However, the steric effect proposed by Sang and Mhin, which causes the structures with $\varphi_{NCCN} = 0°$ to be about 8 kJmol^{-1} higher in energy than those with $\varphi_{NCCN} = 120°$ and 240°, has not been observed.

The relative energies and structural information for the most stable conformers of EDA obtained with the 4-31G* and 6-31G** basis sets are listed in Table 1. In agreement with calculations of Bultinck et al. [11] we observe that the 4-31G* and 6-31G** basis sets do not influence significantly the relative rotational energy profile of EDA in the gas phase, shown in Table 1. Nevertheless, further calculations of the rotational energy profiles of the non-protonated EDA conformers were all done using the more elaborate 6-31G** basis set. Extending the 4-31G* basis set to a 6-31G** basis set lowers the relative energy values of the EDA conformers from about 0.2 to about 1.4 kJmol^{-1}. It lengthens the r_{CC} and r_{NC} bonds by about 0.003 Å. In order to calculate solvent interactions an extended basis set such as 6-31G** is more appropriate.

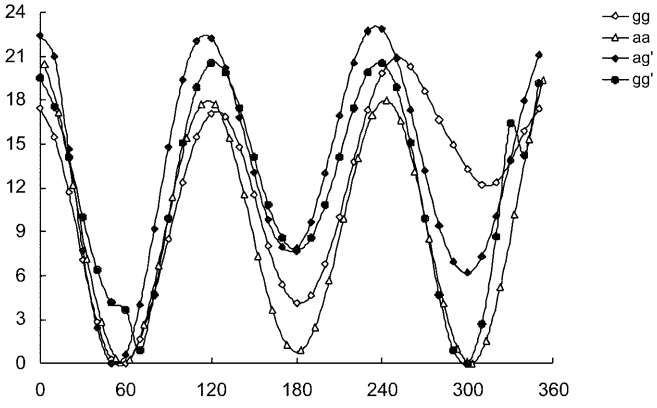

Fig. 2. The rotational energy profiles for the gg, aa, ag′ and gg′ EDA conformers in the gaseous phase are calculated with a 4-31G* basis set and (*BP86*). φ_{NCCN} (degrees) versus energy (kJ mol^{-1}) Perdew's 1986 gradient-corrected functional with Becke's exchange functional

From our calculations with the 4-31G* basis set we notice that the most stable conformations, i.e. aGg′ and gGg′, are gauche with φ_{NCCN} of 55.9° and 62.3° respectively, which correspond to the experimental dihedral angles of 64(5)° and 63(2)° found by Yokozeki and Kuchitsu [2] and Marstok and Mõlendal [3], respectively. r_{CC} bond lengths of 1.541 and 1.531 Å and the bond lengths of r_{NC1}, 1.467 Å, r_{NC2}, 1.471 Å, r_{NC1}, 1.466 Å, and r_{NC2}, 1.475, are in good agreement with the experimental values of 1.545(8) and 1.469(4) Å, respectively. With the 6-31G** basis set we obtained the same stable conformations with φ of 56.4° and 62.5°, r_{CC} bond lengths of 1.543 and 1.534 Å and bond lengths for r_{NC1} of 1.471 Å, for r_{NC2} of 1.470 Å, for r_{NC1} of 1.478 Å and for r_{NC2} of 1.470 Å. Using dielectric measurements, Zahn [4] determined a dipole moment of 1.96 D, which is in agreement with the calculated dipole moment of 2.028 D for the gGg′ conformer.

In EDA, we see that the r_{CC} bond is shorter in the staggered conformer than in the eclipsed conformer and that its length increases with increasing number of lone pairs antiperiplanar to the C—C bond.

The rotational barriers are given in Table 2. The activation barrier energies correspond well to those

Table 2. Rotational activation barriers between two minimum energy states through the transition-state structures of EDA using a 6-31G** basis set and BP86 and second-order Møller–Plesset perturbation theory/6-31G**

	aGa → aAa	gGg → gAg	aGg′ → aAg′	gGg′ → gAg′
E_{rot} (kJ mol^{-1})	17.7	17.4	21.7	20.0
E^{a}_{rot} (kJ mol^{-1})	19.7	20.8	24.3	22.0

[a] Ref. [10]

Table 1. Relative energies and structural information of the conformers for 1,2-ethanediamine (*EDA*) with a 4-31G* and a 6-31G** basis set and (*BP86*) Perdew's 1986 gradient-corrected correlation functional with Becke's exchange functional

	aGa	aAa	aGg′[c]	aAg′	gGg′	gAg′	gGg	gAg	aG′g′	gG′g
ΔE^{a} (KJ mol^{-1})	2.87	3.65	0.00	7.87	2.77	10.58	6.39	11.40	6.45	19.79
r_{CC} (Å)	1.546	1.546	1.541	1.539	1.531	1.532	1.532	1.531	1.539	1.533
r_{CN1} (Å)	1.470	1.470	1.467	1.470	1.466	1.472	1.475	1.471	1.470	1.468
r_{CN2} (Å)	1.470	1.470	1.474	1.469	1.475	1.472	1.475	1.471	1.472	1.468
φ_{NCCN} (degrees)	58.0	180.0	55.9	178.3	62.3	180.0	55.4	−178.5	−57.68	−43.73
Dipole moment (D)	0.080	0.000	2.131	2.430	2.219	0.000	0.173	2.059	2.438	1.677
ΔE^{b} (KJ mol^{-1})	2.27	3.10	0.00	7.13	2.24	9.81	6.15	10.42	5.89	18.42
r_{CC} (Å)	1.549	1.548	1.543	1.541	1.534	1.535	1.535	1.534	1.541	1.536
r_{CN1} (Å)	1.473	1.473	1.471	1.474	1.470	1.475	1.478	1.474	1.473	1.472
r_{CN2} (Å)	1.473	1.473	1.470	1.472	1.478	1.475	1.478	1.474	1.476	1.472
φ_{NCCN} (degrees)	58.2	180.0	56.4	178.2	62.5	175.8	56.2	−177.9	−59.01	−45.85
Dipole moment (D)	0.391	0.000	2.467	2.301	2.028	0.000	0.148	1.992	2.054	1.594

[a] 4-31G* basis set
[b] 6-31G** basis set
[c] The calculated energies for this conformer are −190.32438 (4-31G*) and −190.52569 (6-31G**) hartree

calculated by Sang and Mhin [10], showing that density functional theory is able to reproduce rotational energy profiles of the EDA molecule computed at the second-order Møller–Plesset perturbation theory (MP2)/6-31G** level; however, the absolute values of the activation barrier energies calculated with density functional theory are all about 2 $kJmol^{-1}$ lower than those obtained from the (MP2)/6-31G** calculations.

Single-point calculations using ADF23, a triple-zeta basis set and BP86 were carried out for the most stable EDA conformers. We used the optimal structures obtained previously and calculated the ELF of these conformers. These functions are depicted in Fig. 3. For the aGa conformer we do not observe any hydrogen-bond formation. Comparing the ELF isosurfaces of the lone pairs for aGa with those of aGg′, we observe for the aGg′ conformer that the ELF isosurface of the lone pair pointing to a hydrogen atom of the other amine group is deformed. We can consider this as an indication of weak hydrogen-bond formation, keeping in mind that for the aGg′ conformer the N—HN bond distance is 2.379 Å. The NH bond length is 1.030 Å, as compared to 1.026 Å in an NH bond which is not perturbed. Hydrogen bonding is known to be strong in collinear structures of NH—LN in which the N—HN distance is about 1.9 Å. Thus, in the case of nonprotonated EDA we have, depending on the lone pair orientation, weak hydrogen-bond formation.

Both the LDA and the GGA functionals such as BP86 and the hybrid functional B3LYP were used to calculate the rotational energy profile of the gg EDA. The rotational energy and the r_{CC} and r_{CN} bond lengths as a function of φ_{NCCN} for the Voska–Wilk–Nasair (VWN) functional, BP86 and B3LYP are shown in Fig. 4. As known from the literature, the gradient-corrected calculations tend to lengthen the bonds and increase the energy, whereas the local functionals tend to shorten the bonds and decrease the energy. Comparing the bond lengths obtained from the VWN and BP86 calculations, we notice a bond lengthening of about 0.003 and 0.004 Å for the r_{CC} and r_{NC1} bond lengths, respectively. Results obtained with B3LYP are only 0.002 and 0.003 Å larger for the C—C bond length and the N—C bond length, respectively, compared to the calculations with the local functional. This agrees with the difference of about 0.001 Å between the BP86 and B3LYP calculations and can be attributed to the inclusion of a gradient-dependent-correlation term and a Hartree–Fock exchange term into B3LYP.

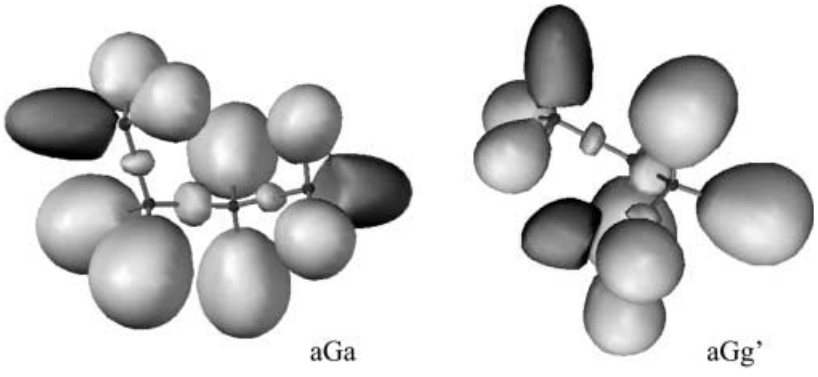

Fig. 3. Three-dimensional representation of the electron localisation function (*ELF*) isosurface with ELF = 0.85 for the aGa and aGg′ nonprotonated EDA conformers. The ELF of the lone pair is *slightly darkened*

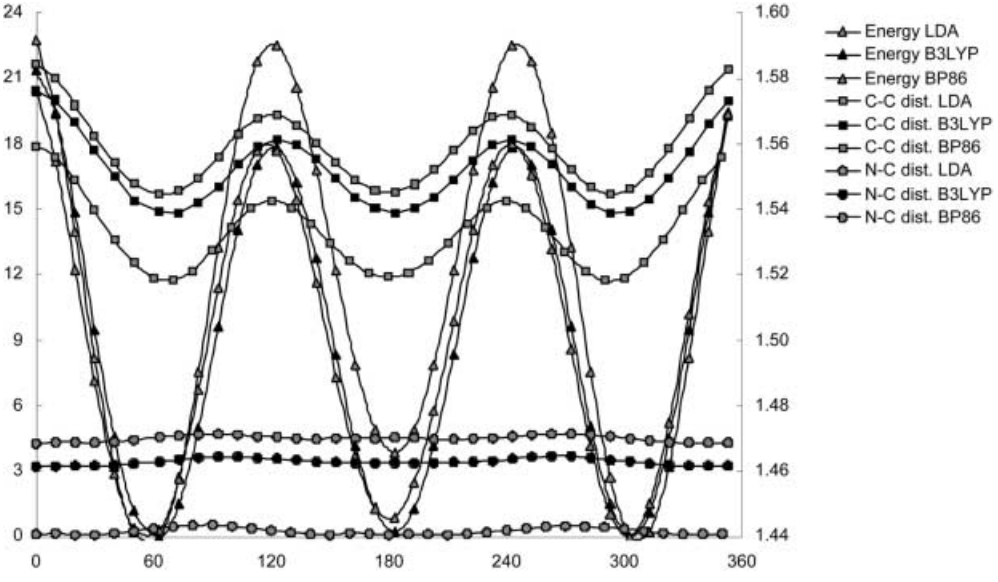

Fig. 4. The rotational energy profiles of the aa EDA conformer in the gas phase calculated with a 6-31G** basis set and the local density approximation (*LDA*), BP86 and Becke's three parameter hybrid method with the Lee, Yang and Parr correlation functional (*B3LYP*). The *x*-axis φ_{NCCN} in degrees, the left *y*-axis has the energy in kilojoules per mole and the right *y*-axis has r_{CC} and r_{NC} bond lengths in angstroms

In order to include solvent effects two different models were used. First, we considered the Onsager SCRF dipole model, where the solute is placed into a spherical cavity. Notice, this method has the advantage of being analytic. The drawback of this approach is that this spherical cavity is not appropriate to describe irregularly shaped molecules in solution. We calculated a cavity with a radius of 6.04 Å. The dielectric constant, ε, of the aqueous solvent was taken as 80.0. The rotational energy profiles of some conformers of EDA are shown in Table 3. The dipole model does not include sufficiently solvent interaction with the EDA molecule, i.e. the change in the dipole moments included by the interaction with the solvent is small. This is also reflected in small energy changes upon introduction of the solvent. As mentioned before, this is due to the nonspherical geometry of EDA; therefore, we considered a more elaborate model, namely the SCIPCM, where a more realistically shaped cavity based on an isodensity surface is considered. An isodensity value of $\rho_{\text{lim.}} = 0.001$ and ε of 80.0 were used in the calculations depicted in Table 4. Notice that owing to the numerical approach to the solvent–solute interactions only single-point calculations were done on the previously optimised most stable EDA conformers. Interactions with the solvent are strong, as shown by the considerable changes in the dipole moments. As a consequence, the relative stability of the EDA conformers changes, making those conformations where the lone pairs are in opposite directions, i.e. with the lone pairs antiperiplanar to the C—C bond, energetically more advantageous. It is clear that through the electrostatic interactions of the continuum model the conformations where the lone pairs are the furthest apart from each other are preferred. Notice that the dipole moments generally increase when taking solvent interactions into account.

The rotational barriers including solvent interactions through the SCRF dipole model and the SCIPCM are given in Table 5. As mentioned earlier, the SCRF dipole model does not change the rotational energy profile of EDA in the gas phase; however, inclusion of solvent interactions by the SCIPCM lowers the rotational energy barriers for the aGa-to-aAa and gGg′-to-gAg′ transitions by 0.8 and 1.8 kJ mol^{-1}, respectively, whereas the values for a rotation from gGg to gAg and aGg′ to aAg′ are increased by 6.3 and 6.5 kJ mol^{-1}. Our calculation clearly shows that the SCIPCM predicts a much larger effect on the solvation. The energy difference of the conformations of lowest energies is smaller. This is in qualitative agreement with NMR measurements, which clearly show four equivalent hydrogen atoms at room temperature due to fast jumps between different conformations and fast proton exchange.

3.2 Monoprotonated EDA

EDA1 has only one lone pair left. In this case there are only two types of conformations arising from different orientations of the lone pair, namely, the a and g conformations. The rotational energy profiles calculated with a 6-31G** basis set and BP86 are shown in Fig. 5. The linear transit calculations were done as described previously. For the two types of N lone pair orientations, we obtain stable structures at φ_{NCCN} dihedral angles of 36°, 180° and 324°. We find transition states for φ_{NCCN} values of 0°, 127° and 233°. The relative energies and the structural information for the conformers of EDA1 calculated in the gas phase and in aqueous solution are listed in Table 6.

Protonation of one of the amine groups elongates the r_{CC} bond by 0.02 Å in comparison to the nonprotonated conformers. The r_{NC} bond in the protonated amine is 0.02–0.05 Å longer than the r_{NC} bond in the nonprotonated one. Notice that increasing the φ_{NCCN} angle leads to a decrease in the r_{CC} bond length and an increase in the r_{NC} bond length. In contrast to the nonprotonated EDA conformers, the most stable EDA1 conformer does not have the shortest r_{CC} bond length.

The rotational barrier in the gas phase for a gauche to an anti conformation transition is about 66.0 kJmol^{-1}, with a transition state at a φ_{NCCN} dihedral angle of 127.3°. This barrier is about 3 times bigger than for the nonprotonated EDA and can be assigned to hydrogen-bond formation.

Inclusion of solvent interaction through the SCIPCM lowers the rotational barrier from 66.0 to 34.6 kJmol^{-1}. This also demonstrates that for the more polarised EDA1, the solute–solvent interactions are more important than for the less polarised EDA.

In order to illustrate the presence of hydrogen-bond formation for EDA1, single-point calculations using ADF23, a triple-zeta basis set and BP86 were done. We used the optimal structures obtained previously and

Table 3. Relative energies using the self-consistent reaction field (*SCRF*) solvent model (a_0 = 6.04 Å and ε = 80.0) for the conformers of EDA with a 6-31G** basis set and BP86

	aGa	aAa	aGg′[a]	aAg′	gGg′	gAg′	gGg	gAg	aG′g′	gG′g
ΔE (kJ mol^{-1})	3.09	3.88	0.00	7.31	2.24	10.71	6.95	10.66	6.04	18.98
Dipole moment (D)	0.400	0.000	2.535	2.254	2.081	0.000	0.154	2.037	2.350	1.636

[a] The calculated energy is −190.52598 hartree

Table 4. Relative energies using the self-consistent isodensity polarisable continuum model (*SCIPCM*) for the conformers of EDA with a 6-31G** basis set and BP86

	aGa[a]	aAa	aGg′	aAg′	gGg′	gAg′	gGg	gAg	aG′g′	gG′g
ΔE (kJ mol^{-1})	0.00	0.53	0.96	5.19	3.69	9.25	8.10	9.25	4.70	17.42
Dipole moment (D)	0.590	0.000	2.919	2.765	2.447	0.000	0.151	2.431	2.783	1.915

[a] The calculated energy is −190.53213 hartree

calculated the ELF of these EDA1 conformers. The functions are depicted in Fig. 6.

On comparing the lone pair (darkened lobe) of the EDA1 conformer with a φ_{NCCN} dihedral angle of 0° and 180°, a clear difference can be seen in the ELF. The ELF surface of the lone pair in the conformer with $\varphi_{NCCN} = 35.9°$ has the typical shape of a bond. For the gauche conformer the N—HN bond distance is 1.66 Å. This is a clear indication of the presence of strong hydrogen bonding for the gauche conformer of EDA1.

Table 5. Rotational activation barriers between two minimum energy states through the transition-state structures of EDA using the SCRF dipole model and the SCIPCM, a 6-31G** basis set and BP86

	aGa → aAa	gGg → gAg	aGg′ → aAg′	gGg′ → gAg′
E_{rot}^{a} (kJ mol^{-1})	17.6	17.2	21.8	20.5
E_{rot}^{b} (kJ mol^{-1})	16.9	19.4	14.2	18.6

[a] SCRF dipole model
[b] SCIPCM

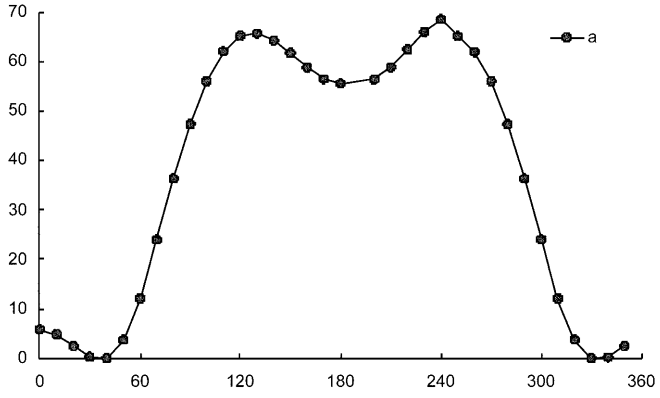

Fig. 5. The rotational energy profile for the g monoprotonated EDA (*EDA1*) conformers in the gaseous phase are calculated with a 6-31G** basis set and BP86. φ_{NCCN} (degrees) versus energy (kJ mol^{-1})

Table 6. Relative energies and structural information of the conformers of monoprotonated EDA (*EDA1*) with a 6-31G** basis set and BP86 in the gaseous phase and in aqueous solution through the SCIPCM

	G → G′	G[c]	G → Δ	G′[c]
ΔE[a] (kJ mol^{-1})	6.01	0.00	66.02	64.51
r_{CC} (Å)	1.587	1.557	1.552	1.545
r_{CN1} (Å)	1.505	1.512	1.533	1.557
r_{CN2} (Å)	1.485	1.481	1.464	1.456
φ_{NCCN} (degrees)	0.0	35.9	127.3	180.0
Dipole moment (D)	4.993	4.624	2.648	3.284
ΔE[b] (kJ mol^{-1})	7.28	0.00	34.59	35.91
Dipole moment (D)	4.648	4.166	2.362	2.420

[a] Gas phase
[b] Aqueous solution
[c] G: gauche conformer; △: anti conformer

We can use our calculations of EDA1 to obtain the PA for nonprotonated EDA in gas phase as follows:

$$PA(EDA) = E(EDA1) + ZPE(EDA1) + TE(EDA1) - E(EDA) - ZPE(EDA) - TE(EDA) \quad (1)$$

where E is the electronic energy, ZPE is the zero-point energy and TE is the thermal energy correction to the enthalpy for nonprotonated EDA and EDA1 molecules. These values were obtained through a vibrational frequency calculation of the aGg′ EDA conformer and the most stable EDA1 with a φ_{NCCN} dihedral angle of 35.9° and are shown in Table 7. This calculated PA of −945.1 kJmol^{-1} is in better agreement with the experimental one than the equivalent value calculated at the (MP2)/6-31G** level [3], which yields −964.5 kJmol^{-1}.

3.3 Diprotonated EDA

In EDA2 both amine groups are protonated. The rotational energy profiles calculated with a 6-31G** basis set and the BP86 functional are shown in Fig. 7. The linear transit calculations were done as described previously. There is a stable structure at a φ_{NCCN} dihedral angle of 180° and a metastable structure at $\varphi_{NCCN} \cong 100°$. We find only one transition state, with a φ_{NCCN} dihedral angle of 0°. The relative energies and structural information for the conformers of EDA2 in the gas phase and in aqueous solution are listed in Table 8.

Protonation of both amine groups elongates the r_{NC} bonds by 0.08–0.09 Å in comparison to the nonproto-

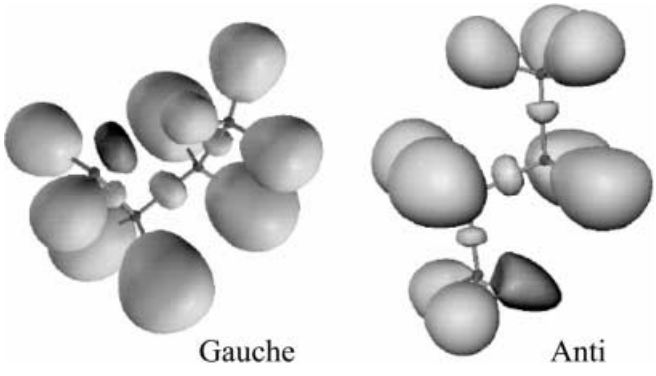

Fig. 6. Three-dimensional representation of the ELF isosurface with ELF = 0.85 for EDA1 with a φ_{NCCN} dihedral angle of 35.9° and 180°. The ELF of the lone pair is *slightly darkened*

Table 7. Proton affinity (PA) of EDA using electronic energy, E, zero-point energy (*2PE*) and thermal energy (*TE*) corrections to the enthalpy for aGg′ nonprotonated EDA and the most stable EDA1 conformer with a 6-31G** basis set and BP86. Energies in kilojoules per mole. *EDA2* is diprotonated EDA

	ΔE	ΔZPE	ΔTE	PA_{calc}	PA_{exp}^{a}
EDA1 → EDA	−1015.4	36.9	33.4	−945.1	−945.2
EDA2 → EDA1	−488.8	38.0	38.8	−412.0	–

[a] Ref. [23]

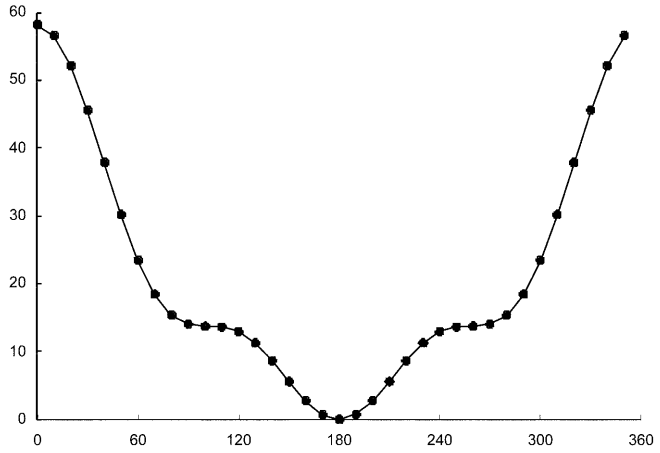

Fig. 7. The rotational energy profile of diprotonated EDA in the gas phase calculated with a 6-31G** basis set and the BP86 exchange functionals. φ_{NCCN} (degrees) versus energy (kJ mol^{-1})

Table 8. Relative energies and structural information for the conformers of EDA2 with a 6-31G** basis set and BP86 in the gaseous phase and in aqueous solution

ΔE^a (kJ mol^{-1})	60.73	0.00
r_{CC} (Å)	1.576	1.547
r_{CN1} (Å)	1.529	1.523
r_{CN2} (Å)	1.546	1.538
φ_{NCCN} (degrees)	0.0	180.0
Dipole moment (D)	12.339	17.970
ΔE^b (kJ mol^{-1})	53.19	0.00
Dipole moment	15.543	18.873

[a] Gas phase
[b] Aqueous solution

nated conformers. At a larger φ_{NCCN} angle, the r_{CC} bond length is increased and the r_{NC} bond length decreases slightly. In agreement with the nonprotonated EDA conformers, the most stable EDA2 conformer has the shortest r_{CC} bond length. The gas-phase rotational barrier for an "anti" to "anti" transition is about 60.7 kJ mol^{-1}, with a transition state structure at $\varphi_{NCCN} = 0°$. This barrier is about 3 times bigger than for nonprotonated EDA and can be ascribed to steric and electrostatic repulsion between the two protonated amine groups. Inclusion of solvent interactions through the SCIPCM lowers the rotational barrier from 60.7 to 53.2 kJ mol^{-1}. Solvation of EDA2 using explicit water molecules [23] lowers the rotational barrier by 22.2 kJ mol^{-1}.

We can use our results for EDA2 to calculate the PA for the EDA1 molecule. Using the adapted formula to calculate the PA (Eq. 1), we predict the PA of EDA1 to be −412.0 kJ mol^{-1}, which is practically half the PA value for nonprotonated EDA.

4 Conclusions

In this work we studied the structures and conformational energies of nonprotonated EDA, EDA1 and EDA2 in the gas phase and in aqueous solution. Structures, conformational energies and PAs of "gas-phase" density functional theory calculations of nonprotonated EDA are in good agreement with experimental data. The results obtained for the EDA1 and EDA2 conformers are completely predictive. EDA1 has a stable conformation for a φ_{NCCN} dihedral angle of 35.9°. The rotational barrier energy is estimated at 66.0 and 34.6 kJ mol^{-1} in the gas phase and in aqueous solution, respectively. The PA for EDA1 was predicted to be −412.0 kJ mol^{-1}. The rotational barrier energy for EDA2 is found to be 60.7 and 53.2 kJ mol^{-1} in the gas phase and in aqueous solution, respectively. ELF calculations show the existence of weak hydrogen bonding for nonprotonated EDA and strong hydrogen bonding for the EDA1 conformers.

Thus, the results of density functional calculations have been shown to be a very useful tool in order to gain more insight into the influence of protonation and solvation on the conformational properties of EDA.

Acknowledgement. This work was supported by the Swiss National Science Foundation.

References

1. Toru T, Sadatsugu O, Nobuhiko K (1985) J Polym Sci 23: 2109
2. Yokozeki A, Kuchitsu K (1971) Bull Chem Soc Jpn 44: 2926
3. Marstok KM, Mõlendal H (1978) J Mol Struct 49: 221
4. Zahn CT (1932) Phys Z 33: 525
5. Carballeira L, Mosquera RA, Rios MA, Tovar CA (1989) J Mol Struct 193: 263
6. Hdjiliadis N, Diot A, Theophanides T (1972) Can J Chem 50: 1005
7. Graffeuil M, Labarre J-F, Leibovici C, Théophanides T (1973) J Chim Phys 70: 1295
8. Radom L, Lathan WA, Hehre WJ, Pople JA (1973) J Am Chem Soc 95: 693
9. Kazerouni M, Hedberg L (1994) J Am Chem Soc 116: 5279
10. Sang JL, Mhin BJ (1994) J Phys Chem 98: 1129
11. Bultinck P, Goeminne A, Van de Vondel D (1995) J Mol Struct 339: 1
12. Chang Y-P, Su T-M, Li T-W, Chao I (1997) J Phys Chem A 101: 6107
13. Boudon S, Wipff G (1991) J Mol Struct 228: 61
14. Becke AD, Edgecombe NE (1990) J Chem Phys 92: 5397
15. Savin A, Nesp R, Wengert S, Fässler TF (1997) Angew Chem Int Ed Engl 36: 1808
16. Frisch MJ, Trucks GW, Schlegel HB, Gill PMW, Johnson BG, Robb MA, Cheeseman JR, Keith TA, Petersson GA, Montgomery JA, Raghavachari K, Al-Laham MA, Zakrewski VG, Ortiz JV, Foresman JB, Cioslowski J, Stefanov BB, Nanayakkara A, Challacombe M, Peng CY, Ayala PY, Chen W, Wong MW, Andres JL, Replogle ES, Comperts R, Martin RL, Fox DJ, Binkley JS, Defrees DJ, Baker J, Stewart JP, Head-Gordon M, Gonzalez G, Pople JA (1995) Gaussian 94. Gaussian, Pittsburgh, Pa
17. (a) Baerends EJ, Ellis DE, Ros P (1973) Chem Phys 2: 41; (b) Baerends EJ, te Velde BJ (1992) J Comput Phys 99: 84
18. Vosko SH, Wilk L, Nusair M (1980) Can J Phys 58: 1200
19. (a) Perdew JP (1986) Phys Rev B 33: 8822; (b) Becke AD (1988) Phys Rev A 38: 3098
20. Becke AD (1993) J Chem Phys 98: 5648
21. Wong MW, Frisch MJ, Wiberg KB (1991) J Am Chem Soc 113: 4776
22. (a) Tawa GJ, Martin RL, Pratt LR, Russo TV (1996) J Phys Chem 100: 1515; (b) Craw JS, Guest JM, Cooper MD, Burton NA, Hillier IH (1996) J Phys Chem 100: 6304
23. Yamabe S, Hirao K, Wasada H (1992) J Phys Chem 96: 10261